Lightning Phenomenology Notes

Note 10

9 March 1983

THE EFFECT OF PROPAGATION ON ELECTROMAGNETIC FIELDS RADIATED BY LIGHTNING

Louis Baker and Robert L. Gardner

Mission Research Corporation

ABSTRACT

The model of Gardner (Radio Science 16, 377-384, 1981) is used to study the attenuation of lightning fields with distance over a variety of propagation paths. The lightning channel may consist of an arbitrary arrangement of linear segments, each with a different propagation velocity. The effects of an imperfectly conducting, anisotropic ionosphere and a lower surface of earth or water (including sea state) are studied.

It is of great interest to deduce the properties of lightning, such as the current profile as a function of time, from remote measurements of the radiated fields. For this reason, distortion of the signal by propagation path effects must be understood quantitatively. The study of the distortion of electromagnetic transient fields as they propagate over the earth's surface has a long history; Sommerfeld (Ref. 1) considered the propagation of radio waves over an imperfectly conducting earth in 1909, and a number of recent texts (Refs. 2, 3, 4) review more recent developments. In general the signals are attenuated, the attenuation increasing with frequency and decreasing as the surface conductivity increases. This presupposes smooth surfaces; corrugated surfaces (Refs. 5, 6, 7) have also been studied in connection with propagation over a sea surface covered by waves. When the ocean waves have lengths small compared to the radio wavelength, a "trapping" of the surface wave is possible (Ref. 8) which results in an increase in signal, while at higher frequencies an increased attenuation results. The attenuation does not increase monotonically with frequency, as Barrick (Ref. 7) notes, but rather a saturation sets in, with the greatest losses for frequencies in the range 10 to 15 MHz for typical ocean wave spectra.

In this paper we use the computer model developed by Gardner (Refs. 9, 10), extended using the results of Barrick (Ref. 6), to evaluate the role of propagation effects on lightning signals.

THEORY

First we will briefly review the theory; a more complete discussion will be found in References 2 through 10. The lightning channel is treated as a dipole source with specified current, with triple exponential form:

$$I(t) = \left[A(\exp(-at) - \exp(-bt)) + B\exp(-ct)\right] U(t) \quad (1)$$

where U(t) is the Heaviside step function, A = 30 kA, B = 2.5 kA, a = $2 \times 10^4\ s^{-1}$, b = $2 \times 10^5\ s^{-1}$, c = $1. \times 10^3\ s^{-1}$. The term proportional to A has an inverse rise time of roughly b, or about 10 microseconds, and a fall time of roughly 1/a or about 100 μs. The term proportional to B represents the "continuing current" and constitutes a slow "tail" to the current pulse, falling off over several milliseconds. While such a form for I(t) is not perfect (e.g., its behavior at t=0), it is often used (Ref. 12) and we will follow custom for ease of comparison with other references. This current waveform propagates along the channel with normalized velocity v, where v = speed of light divided by the velocity of propagation, i.e., v is always greater than 1.

We will work in frequency domain rather than time domain, and assume the fields have time dependence exp $(i\omega t)$. This will both facilitate analysis and comparison with observation. We can in principle inverse Fourier transform into time domain if desired. The lightning channel is treated as a chain of dipole sources, and the Hertz potential (Ref. 13) may then be used to find the fields at any point. The Hertz vectors have simpler expressions in terms of the sources than the vector and scalar potentials and therefore simplify calculations. For example, the electric field due to a vertical electric dipole dipole may be written in terms of the vertical component of the electric Hertz vector as:

$$\vec{E} = \nabla\nabla \cdot \Pi + k^2\Pi \qquad (2)$$

where π is the Hertz vector and $k = \omega/c$ is the wavenumber. Expressions for general dipole source orientation will be found in Baños (Ref. 2). Cylindrical coordinates (ρ,ϕ,z) will be used (Ref. 10), with the source centered above the origin, as shown in Figure 1. Wait (Refs. 7, 8) shows that the Hertz vector due to a vertical dipole at any point above the surface may be written as:

$$\pi = \frac{Ids}{4\pi i\epsilon\omega} \int_0^\infty \Big[\exp[-u|z+h|] + R(\lambda)$$

$$\exp[-u(z-h)]\Big] \frac{\lambda}{u} J_0(\lambda\rho)d\lambda \qquad (3)$$

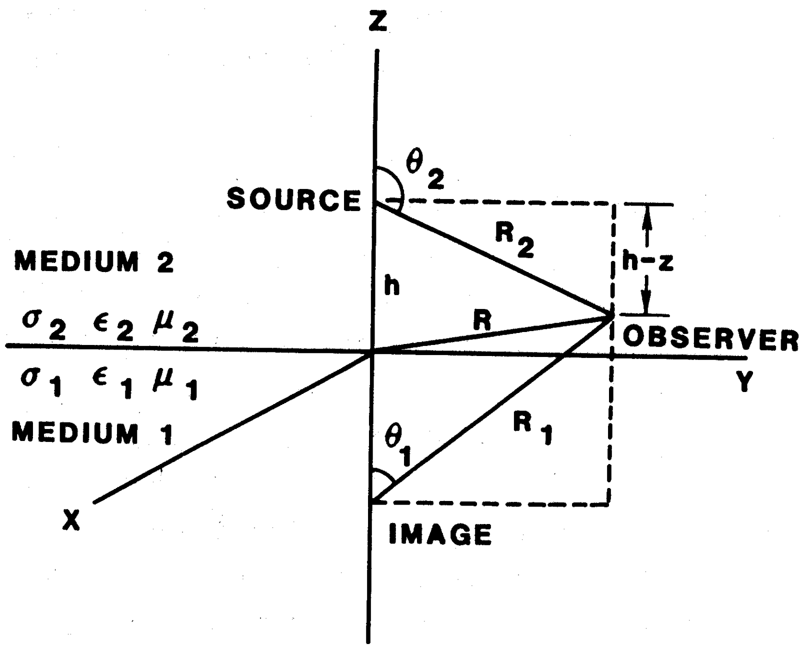

Figure 1. Geometry for a point source.

where c the speed of light, ds is the length of the dipole carrying current I (resulting in a current moment of Ids), $u = (\lambda^2 - k^2)^{\frac{1}{2}}$, and

$$R(\lambda) = \frac{u - ik\Delta}{u + ik\Delta} \tag{4}$$

is a reflection coefficient, expressed in terms of the normalized surface impedance Δ which we will define shortly. By use of the identity

$$\exp(- ikr)/r = \int_0^\infty \exp[-u(h-z)] \, J_0(\lambda\rho)d\lambda \tag{5}$$

where

$$r = (\rho^2 + (h-z)^2)^{\frac{1}{2}}$$

We may put this in the form:

$$\Pi = \frac{Jds}{4\pi i\varepsilon\omega}\left[\frac{e^{ikr'}}{r'} + \frac{e^{-ikr}}{r} - 2P\right] \tag{6}$$

with

$$r = (\rho^2 + (z-h)^2)^{\frac{1}{2}}$$

$$r' = (\rho^2 + (z+h)^2)^{\frac{1}{2}}$$

$$P = \int_0^\infty \frac{ik\Delta \; \exp - u(h-z)}{u_0 + ik\Delta} \frac{\lambda}{u} J_0(\lambda\rho)d\lambda \tag{7}$$

and Π the z component of the Hertz vector. We clearly have a direct wave of the form:

$$\Pi_d = Ids/(4\pi i\varepsilon\omega) \exp(ikr)/r \tag{8}$$

with a reflected wave:

$$\Pi_r = Ids/(4\pi i\varepsilon\omega)[\exp(ikr')/r' - 2P] \tag{9}$$

(where r' is the distance to the image dipole source). Note that for a perfectly conducting, smooth ground P=0. The quantity $\Delta = Z/\eta$ in the above is the surface impedance normalized by the free space value $\eta = 120\ \Omega$. The surface impedance is the wave impedance, that is the ratio of fields Z = E/H, at the surface. For a smooth homogeneous surface it is given by:

$$\Delta = u_1/(\sigma_1 + i\varepsilon_1\omega) \tag{10}$$

where

$$u_1 = (k^2 - k_1^2)^{\frac{1}{2}} \quad , \; k_1 = (\omega^2\mu_1\varepsilon_1 - i\omega\mu_1\sigma_1)^{\frac{1}{2}} \tag{11}$$

k_1 as the wavenumber below the surface, ω the frequency, σ_1 the conductivity, ε_1 and μ_1 the dielectric permittivity and the permeability, respectively, with References 6, 7 giving corrections for corrugations. Note that it is in general a complex number; the real part represents a resistive component while the imaginary part represents a reactance and gives rise to the wave trapping discussed previously. The integral may be evaluated using the asymptotic methods, yielding an expression containing the complex error function. We found it simplest and most accurate to include the results of Reference 6 by simply calculating the transmission for a smooth surface and then correcting this result for the changed attenuation, interpolating from a table in frequency, range, and sea state from the results of Barrick. His data show little effect below frequencies of 3 MHz for propagation ranges below 50 km. Enhancements in signal due to trapping are typically only fractions of a dB for such ranges and are therefore much smaller than other effects. Finally, integrating along the length of the finite channel segments, taking into account the finite signal velocity, results in the factor ds being replaced by terms of the form

$$L\,\mathrm{sinc}(kL/2\ (v - \nabla r)_z) \tag{12}$$

where L is the length of the segment, and V = v/c is the normalized propagation velocity and sinc(z) = sin(z)/z.

We will refer to the signal discussed above as the "ground wave". In addition, there is a "sky wave" due to reflection by the ionosphere. Its treatment is analagous, the "single bounce" approximation of Wait (Ref. 11) being used to find the reflection coefficient. References 9 and 10 give the details of the method used. The sky wave is typically unimportant except at the lowest frequencies. Finally, we note that at frequencies below 1 kHz it is most appropriate to treat the propagation as occurring in a waveguide formed by the ground and the ionosphere. This is discussed in Reference 9 and will not be discussed here.

RESULTS

Figure 2 compares the results of Reference 13 with our calculations, for a pulse propagating at the speed of light along a vertical channel with a length of 1500 m at a distance of 50 km. We show results for propagation over moist ground (the lowest curve), calm sea, and sea in "sea state 6", corresponding to a wind of 30 knots. We note that agreement with the propagation over water is excellent for frequencies below 10 MHz. It would seem that the assumed form for the current I(t) possesses too high a content of high frequencies, possibly due to the "continuing current" term which is discontinuous near t=0. Note that attenuation over the land is somewhat higher than over the highly conductive sea water, but that this is significant only for the higher frequencies. Note also that sea state has an almost indiscernable effect.

Figures 3 and 4 present results for similar calculations for a tortuous channel, both for pulses propagating at the velocity of light and 1/3 that velocity. As the travel time of the pulse down the channel increases, due either to the lengthening of the channel or the slowing of the propagation

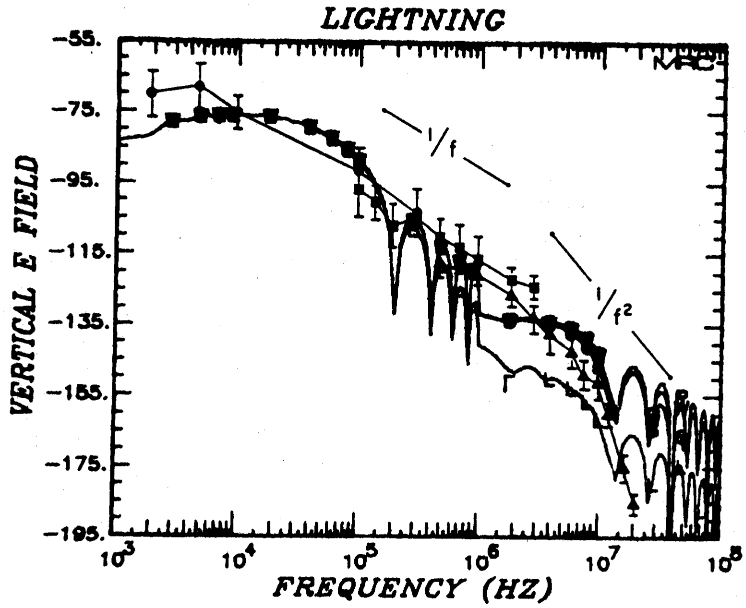

Figure 2. Vertical electric field just above the surface, as a function of frequency, for a vertical channel 1500 m long, carrying the standard current pulse propagating along the channel at the speed of light. The curves are, from bottom to top, for propagation over moist ground, ocean water in sea state six, and a smooth ocean surface.

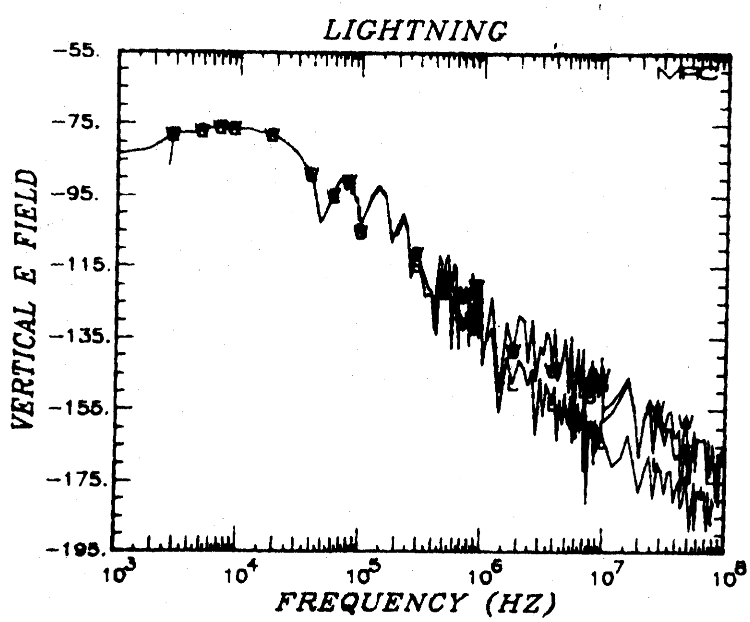

Figure 3. Same as Figure 2, but for a channel with three straight line segments connecting the following points in Cartesian coordinates: (0,0,0), (500,500,500), (-500,-500,1000), (0,0,1500) where all lengths are in meters.

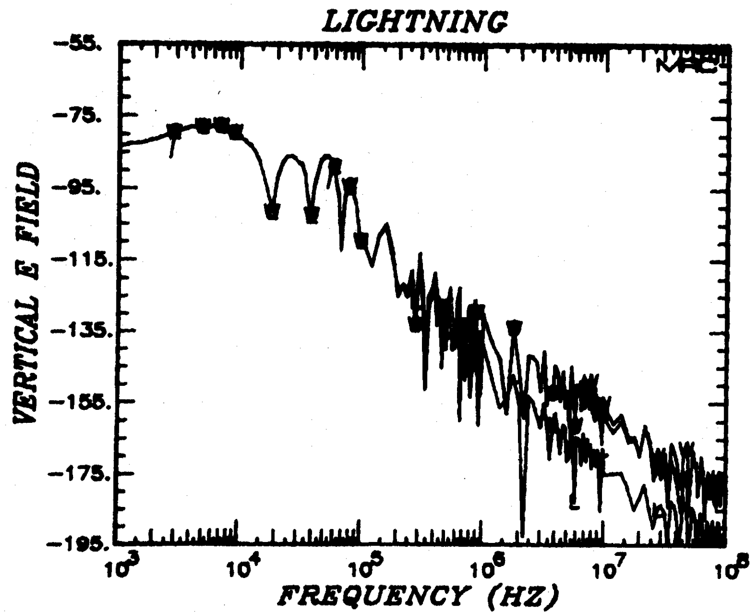

Figure 4. Same as Figure 2, but for a current pulse along the channel with a propagating velocity of 1/3 the speed of light.

along the channel, the resonances shift downward in frequency and the structure of nulls in the $E(\omega)$ curve shifts downward. The slower propagation velocity reduces the high frequency component somewhat. Hence the gross features of the curve, along with the location of the resonances in frequency space, tell us the gross properties of the stroke--its length and propagation velocity. Note that we do not include effects of branching, there being only one current-carrying channel, although it need not be a straight line. Additional branches can be treated with a fairly straightforward modification of the code, however.

Unfolding the pulse shape would be quite a bit more difficult. The pulse shape may be expected to change with propagation (Ref. 9). The pulse shape and the precise geometry of the channel would interact to give the fine structure of $E(\omega)$ at higher frequencies. We could hope to extract the current as a function of space and time only with both optical measurements to supply channel geometry and an array of electromagnetic observations to enable us to separate signals from different portions of the stroke. Note that even the rolloff of signal with frequency is a function of both propagation velocity and pulse shape, and therefore it would be useful if the optical observations would give us the former. There is some hope that in the near future experiments in New Mexico may provide us with such correlated measurements.

REFERENCES

1. A. Sommerfeld, "Uber die Ausbreitung der Wellen in der drahtlose Telegraphie", Ann. Physik 28, 665-737 (1909).

2. A. Baños, Jr., "Dipole Radiation in the Presence of a Conducting Half-Space," Oxford: Pergamon Press, 1966.

3. J. R. Wait, "Electromagentic Waves in Stratified Media," New York: Pergamon Press, 1970.

4. J. R. Wait, "Wave Propagation Theory", New York: Pergamon Press, 1981.

5. D. E. Barrick, "Theory of HF and VHF propagation across the rough sea, 1, The effect of surface impedance for a slightly rough highly conducting medium at grazing incidence", Radio Science 6, pp. 517-526, 1971.

6. D. E. Barrick, "Theory of HF and VHF propagation across the rough sea, 2, Application to HF and VHF propagation above the sea," Radio Science 6, pp. 527-533, 1971.

7. J.R. Wait, "Perturbation analysis for reflection from two-dimensional periodic sea waves," Radio Science 6, pp. 387-391, 1971.

8. J. R. Wait, "Electromagnetic Surface Waves," in Advances in Radio Research, J. A. Saxton, ed., Vol. 1, pp. 157-217, New York: Academic Press, 1964.

9. R. L. Gardner, "A model of the lightning return stroke," Thesis, U. of Colorado, 1980, also as Lightning Phenomenology Notes 6 and 7.

10. R. L. Gardner, "Effect of the propagation path on lightning-induced transient fields," Radio Science 16, pp. 377-384, 1981.

11. J. R. Wait, "Introduction to the theory of VLF propagation," Proc. IRE, 50, pp. 1624-47, 1962.

12. D. M. LeVine and R. Meneghini, "Electromagnetic fields radiated from a lightning return stroke: Application of an exact solution to Maxwell's equations," J. Geophys. Res., 83(c5), 2377-84, 1978.

13. J. B. Marion, "Classical Electromagnetic Radiation," New York: Academic Press, 1965, pp. 227ff.

14. M. A. Uman and P. Krider, "A Review of Natural Lightning: Experimental Data and Modeling," IEEE Trans. Electromag. Compat., EMC-24, pp. 79-111, 1982.